Table IV
Glass Temperature, Viscosity, and Free Volume of the PMMA/MMA System as a Function of Conversion (at 70 °C)

$V_p(X)$	T_g, °C	η, cP	V_f	I_F (ϕ_F)
0	−102.8			8
0.43	−46.2	0.1		10.5
0.48	−37.5	0.195		11
0.53	−28	0.45		12
0.60	−13.7	1.93		14
0.65	−3.0	7.15	0.073	17 (0.0048)
0.67	2.2	14.8	0.0695	22 (0.00625)
0.68	4.5	20.7	0.0672	32 (0.0091)
0.70	9.6	46.23	0.0634	53 (0.015)
0.72	14.2	100	0.0595	73 (0.021)
0.74	20.0	305		75
0.78	31.2	3700		83
0.82	43.2	1.2×10^5		86
0.87	59.5	1.2×10^8		87
0.89	66.4	7.5×10^9		88
0.90	70.0	1×10^{11}		88
0.95	89			
1.0	110			

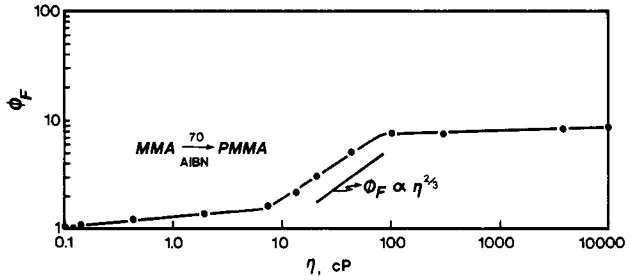

Figure 10. Dependence of fluorescence yield of **2** (at 70 °C) on PMMA/MMA mixture viscosity.

as the viscosity changes from 10 to 100 cP. The slope of this portion of the plot corresponds to $\phi_F \alpha \eta^{2/3}$, which agrees well with the Förster and Hoffmann[13] model. Further increase in conversion leads to a rapid rise in viscosity, as the glassy state is approached, with no further increase in fluorescence. The polymerization region in which fluorescence intensity increases abruptly seems to correpond to the increase of medium viscosity from fluid to rigid glass. This accounts for the abrupt increase in fluorescence until the limiting conversion is reached, at which point fluorescence levels off.

Acknowledgment. The author thanks Drs. S. Balke and K. O'Driscoll for stimulating discussions and gratefully acknowledges the anonymous referees, who made thorough critical and constructive comments.

References and Notes

(1) Balke, S. T.; Hamielec, A. E. *J. Appl. Polym. Sci.* **1973**, *17*, 905.
(2) Friis, N.; Hamielec, A. E. *ACS Symp. Ser.* **1976**, *24*, 82.
(3) Cardenas, J. N.; O'Driscoll, K. F. *J. Polym. Sci., Part A-1* **1976**, *14*, 883. *Ibid.* **1977**, *15*, 1883, 2097.
(4) Dionisio, J.; Mahabadi, H. K.; O'Driscoll, K. F. *J. Polym. Sci., Part A-1* **1979**, *17*, 1891.
(5) Turner, D. T. *Macromolecules* **1977**, *10*, 221.
(6) Lee, H. B.; Turner, D. T. *Macromolecules* **1977**, *10*, 226.
(7) Marten, F. L.; Hamielec, A. E. *ACS Symp. Ser.* **1980**, *104*, 43.
(8) Loutfy, R. O.; Law, K. Y. *J. Phys. Chem.* **1980**, *84*, 2803.
(9) Carsey, T. P.; Findley, G. L.; McGlynn, S. P. *J. Am. Chem. Soc.* **1979**, *101*, 4502, 4511.
(10) Grabowski, Z. R.; Rotkiewicz, K.; Siemiarczuk, A.; Cowley, D. J.; Baumann, W. *Nouv. J. Chim.* **1979**, *3*, 443.
(11) Doolittle, A. K. *J. Appl. Phys.* **1952**, *23*, 236.
(12) Johnson, G. E. *J. Chem. Phys.* **1975**, *63*, 4047.
(13) Förster, Th.; Hoffmann, G. *Z. Phys. Chem.* (*Wiesbaden*) **1971**, *75*, 63.
(14) Tredwell, C. J.; Keary, C. M. *Chem. Phys.* **1979**, *43*, 307.
(15) Taylor, J. R.; Adams, M. C.; Sibbett, W. *Appl. Phys.* **1980**, *102*, 847.
(16) Jaraudias, J. *J. Photochem.* **1980**, *13*, 35.
(17) Baker, R. H.; Gratzel, M. *J. Am. Chem. Soc.* **1980**, *102*, 847.
(18) Karstens, T.; Koh, K. *J. Phys. Chem.* **1980**, *84*, 1871.
(19) Jones, G.; Jackson, W. R.; Halpern, A. M. *Chem. Phys. Lett.* **1980**, *72*, 391.
(20) Eisenbach, C. D. *Photogr. Sci. Eng.* **1979**, *23*, 183.
(21) Bueche, F.; Kelley, F. N. *J. Polym. Sci.* **1961**, *L*, 549.
(22) Bueche, F. "Physical Properties of Polymers"; Interscience: New York, 1962; Chapter 5.

Magic-Angle Carbon-13 Nuclear Magnetic Resonance Study of the Compatibility of Solid Polymeric Blends

E. O. Stejskal, Jacob Schaefer,* M. D. Sefcik, and R. A. McKay

Monsanto Company, Physical Sciences Center, St. Louis, Missouri 63166.
Received May 5, 1980

ABSTRACT: A theoretical analysis of coupled relaxation processes has been used in the quantitative interpretation of carbon-resolved, proton $T_{1\rho}$ data obtained at 15.1 MHz for a variety of solid blends of poly(phenylene oxide) and polystyrene. This analysis permits an estimate of spin-diffusion rates between different chemical species. These rates are strongly dependent on spatial proximity and hence are applicable to the determination of the homogeneity of the blends. Proton $T_{1\rho}$'s in the blends are nearly but not quite averaged to a single value by spin diffusion, indicating extensive intermixing of poly(phenylene oxide) and polystyrene chains. The proton $T_{1\rho}$ experiments are sensitive enough to distinguish between identically prepared blends made from poly(phenylene oxide) and either atactic or isotactic polystyrenes. While the bulk of both types of blends is an intimate mixture of polymer chains, there are also some small regions in the atactic polystyrene blend where the polystyrene is not uniformly dispersed.

Introduction

Magic-angle cross-polarization ^{13}C NMR of nominally homogeneous glassy polymers provides information about both structure and dynamics.[1] Resolved isotropic chemical shifts identify chemical environments, which, as for the frozen conformations of a polymer, may be unique to the solid state. Relaxation experiments exploit this high resolution so that ^{13}C T_1's and $T_{1\rho}$'s can be used to characterize individual main- and side-chain motions in the megahertz- and kilohertz-frequency ranges, respectively.

The high-resolution magic-angle techniques used to obtain ^{13}C NMR spectra in solids can also be employed

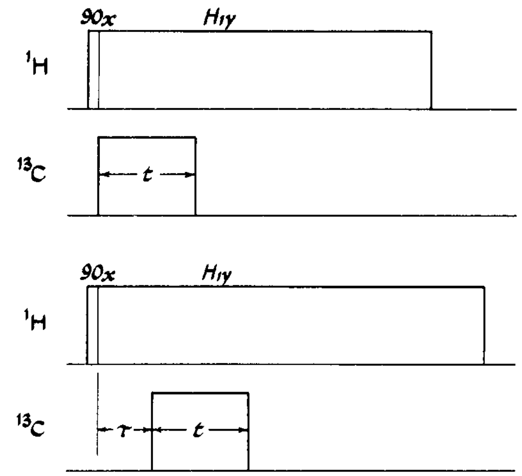

Figure 1. Two cross-polarization pulse sequences.

to measure individual $T_{1\rho}$'s for *protons* attached to different kinds of carbons. This is possible because the final evolution of the carbon signal in a cross-polarization experiment tracks the $T_{1\rho}$ decay of the protons. Neither the cross relaxation between carbons and protons nor the strong homonuclear coupling between protons (10–20 kHz) is affected by a relatively slow (2 kHz) mechanical spinning.[1] Through spin diffusion, proton $T_{1\rho}$'s of a multicomponent system are strongly dependent on the short-range (1 nm) spatial proximity, or mixing, of the various components. Measuring a proton $T_{1\rho}$ by monitoring a resolved carbon resonance is therefore well suited to the analysis of the complicated class of polymeric solids known as blends.[2] In this paper we report the results of such high-resolution ^{13}C NMR experiments on poly(phenylene oxide)/polystyrene (PPO/PS) blends, which lead to new qualitative conclusions regarding both the intimacy and homogeneity of mixing of individual poly(phenylene oxide) and polystyrene chains in these materials.[3]

Experiments

The polymers used in this study were poly(2,6-dimethyl-*p*-phenylene oxide) (Aldrich lot 03, MW = 37 500, M_w/M_n = 1.60), polystyrene (Monsanto lot DR-14, MW = 245 600, M_w/M_n = 2.06), polystyrene (Waters Associates lot 7b, MW = 35 000, M_w/M_n = 1.05), isotactic polystyrene, (i-PS) (Polysciences, MW = 335 000, M_w/M_n = 2.15), poly(*p*-chlorostyrene) (*p*-Cl-PS) (Polysciences, lot 2-1972), and polystyrene-d_8 polymerized from 98 atom % styrene-d_8. The homopolymers and polyblends were prepared by dissolution of the required materials in chloroform followed by precipitation in methanol. The dried powders were then compression molded near 270 °C for 10 min as thin films and subsequently quenched in ice water. Samples prepared in this fashion were clear and void free. Mechanical loss spectra of the PPO/PS blends were consistent with a homogeneous material.[2] The blend of PPO with *p*-Cl-PS was annealed at 70 °C (well below T_g of either component) for 300 h in an air oven; this blend was examined by NMR both before and after annealing.

Disks were punched from the 10-mil films and stacked to fill the magic-angle rotor. Carbon-13 magic-angle spinning results were obtained at 15.1 MHz, using a Beams-Andrew design rotor (0.7-cm^3 sample volume) and spinning speeds of the order of 2 kHz. Samples occupied approximately two-thirds of the volume of the double-tuned coil. Carbon and proton H_1's of 37 kHz and standard radio-frequency and four-phase quadrature routing schemes were employed throughout.[4] The cross-polarization pulse sequence used in the experiments is shown in Figure 1 (top).

Results

The magic-angle ^{13}C line shapes of the minor components of PPO/PS blends are distinctly different from those of the corresponding homopolymers. The low-field shoulder of the aliphatic main-chain carbon resonance of PS in a 75/25 (by weight) PPO/PS blend is enhanced relative to the homopolymer line shape (Figure 2). Similarly, the protonated aromatic-carbon doublet of PPO (δ_c 115) is broadened and considerably more complex in a 25/75 blend than in the homopolymer (Figure 3). This observation is, in fact, easier to make on a blend with PS-d_8, which avoids the strong aromatic PS resonance at δ_c 125. *Inter*chain carbon–deuterium dipolar interactions are negligible.

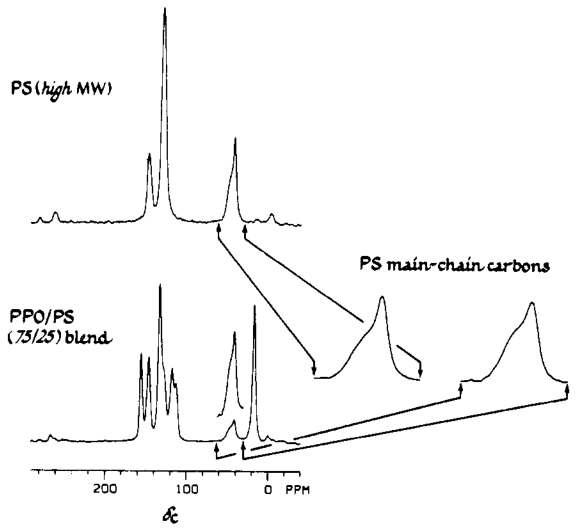

Figure 2. Magic-angle cross-polarization ^{13}C NMR spectra of polystyrene (top) and a 75/25 PPO/PS blend (bottom).

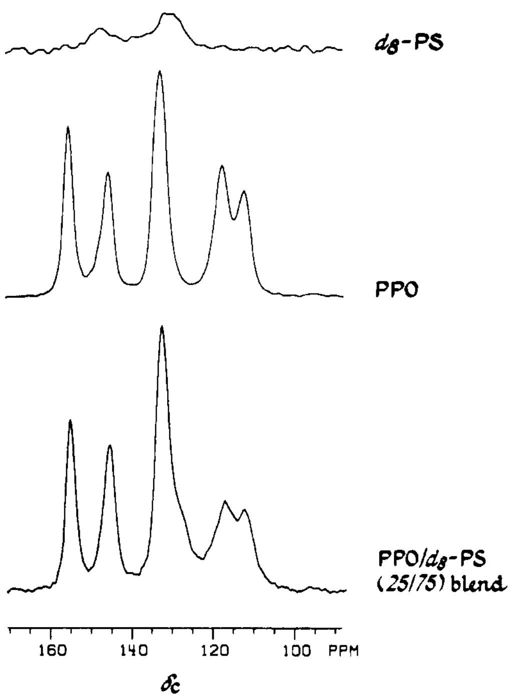

Figure 3. Magic-angle cross-polarization ^{13}C NMR spectra of the aromatic-carbon regions of polystyrene-d_8 (top), poly(phenylene oxide) homopolymer (middle), and a 25/75 blend of the two polymers (bottom).

Proton $T_{1\rho}$ relaxation can be characterized by means of matched spin-locked, cross-polarization transfer experiments.[1,5] After the initial, rapid buildup of carbon polarization, the carbon signal tracks the polarization in the proton reservoir and thus follows its decrease via the $T_{1\rho}$(H) process. Under high-resolution conditions, the individual carbon resonances follow the protons to which they are most closely coupled and thus are capable of resolving $T_{1\rho}$(H) differences between protons which might be difficult to detect if the $T_{1\rho}$(H) process were obtained directly from the composite proton signal.[6] With the pulse sequence of Figure 1 (top), the carbon magnetization, S, is given by[5]

$$\frac{\mathrm{d}S}{\mathrm{d}t} = \frac{S_0 e^{-t/T_{1\rho}(\mathrm{H})} - S}{T_{\mathrm{IS}}} - \frac{S}{T'_{\rho\mathrm{L}}} \tag{1}$$

where S_0 is the maximum carbon polarization available in a matched spin-lock experiment with no dissipative processes, $T_{1\rho}$(H) is the proton rotating-frame spin–lattice relaxation time constant, T_{IS} is the proton–carbon matched spin-lock cross-polarization time constant, and $T'_{\rho\mathrm{L}}$ is the carbon rotating-frame spin–lattice relaxation time constant in the presence of dipolar decoupling of the protons. Thus

$$S = (S_0/T_{\mathrm{IS}})\frac{e^{-t/T_{1\rho}(\mathrm{H})} - e^{-t(1/T_{\mathrm{IS}}+1/T'_{\rho\mathrm{L}})}}{1/T_{\mathrm{IS}} + 1/T'_{\rho\mathrm{L}} - 1/T_{1\rho}(\mathrm{H})} \tag{2}$$

and since $T'_{\rho\mathrm{L}} \gg T_{\mathrm{IS}}$ we can make the approximation

$$S \approx (S_0/T_{\mathrm{IS}})\frac{e^{-t/T_{1\rho}(\mathrm{H})} - e^{-t/T_{\mathrm{IS}}}}{1/T_{\mathrm{IS}} - 1/T_{1\rho}(\mathrm{H})} \tag{3}$$

In addition, since $T_{1\rho}(\mathrm{H}) > T_{\mathrm{IS}}$ when $t \gg T_{\mathrm{IS}}$

$$S \sim S_0 e^{-t/T_{1\rho}(\mathrm{H})}/(1 - T_{\mathrm{IS}}/T_{1\rho}(\mathrm{H})) \tag{4}$$

Thus, from a semilog plot of S vs. t, we obtain $T_{1\rho}$(H).

This method is insensitive to the $T_{1\rho}$(H) relaxation which occurs during the initial cross-polarization process. An alternative method for obtaining $T_{1\rho}$(H) involves a fixed contact time used after a variable delay following the proton spin-locking process (Figure 1, bottom). In this situation

$$\frac{\mathrm{d}S}{\mathrm{d}t} = \frac{S_0 e^{-(t+\tau)/T_{1\rho}(\mathrm{H})} - S}{T_{\mathrm{IS}}} - \frac{S}{T'_{\rho\mathrm{L}}} \tag{5}$$

$$S = (S_0 e^{-\tau/T_{1\rho}(\mathrm{H})}/T_{\mathrm{IS}})\frac{e^{-t/T_{1\rho}(\mathrm{H})} - e^{-t(1/T_{\mathrm{IS}}+1/T'_{\rho\mathrm{L}})}}{1/T_{\mathrm{IS}} + 1/T'_{\rho\mathrm{L}} - 1/T_{1\rho}(\mathrm{H})} \tag{6}$$

As before

$$S \approx (S_0 e^{-\tau/T_{1\rho}(\mathrm{H})}/T_{\mathrm{IS}})\frac{e^{-t/T_{1\rho}(\mathrm{H})} - e^{-t/T_{\mathrm{IS}}}}{1/T_{\mathrm{IS}} - 1/T_{1\rho}(\mathrm{H})} \tag{7}$$

and

$$S \sim \frac{S_0 e^{-(t+\tau)/T_{1\rho}(\mathrm{H})}}{1 - T_{\mathrm{IS}}/T_{1\rho}(\mathrm{H})} \tag{8}$$

when $t \gg T_{\mathrm{IS}}$. If the contact time t is made short, relaxation behavior for small values of τ yields the initial part of the $T_{1\rho}$(H) decay. We choose not to use this method in our experiments because of the fear that a short contact time would not necessarily capture a representative carbon polarization. With long contact times the two methods are equivalent.

Figure 4 displays $T_{1\rho}$(H) relaxation as detected by the protonated, main-chain carbons of PPO, high molecular weight atactic PS, isotactic PS, and three PPO/PS (75/25) blends. The protons were spin locked in a field of 37 kHz. The initial cross polarization was complete within several hundred microseconds so that the first points shown (at 2 ms) are fully indicative of the $T_{1\rho}$(H) process. It can be observed in the blends that the PPO and PS carbons detect slightly different $T_{1\rho}$(H) processes and further that the PS decays are clearly not first order. Thus we have detected considerable but not complete averaging by spin diffusion of the $T_{1\rho}$(H)'s for the two polymers in the blends. We discuss below whether the curvature in the PS decays is due to incomplete spin diffusion or phase separation. For the PS homopolymers, $T_{1\rho}$(H)'s detected by the protonated main-chain and side-chain carbons differ by no more than 5%. Values for all $T_{1\rho}$(H)'s are presented in Tables I and II. For curved relaxation plots the (nominal) initial slope, indicated by brackets, is different from the final slope.

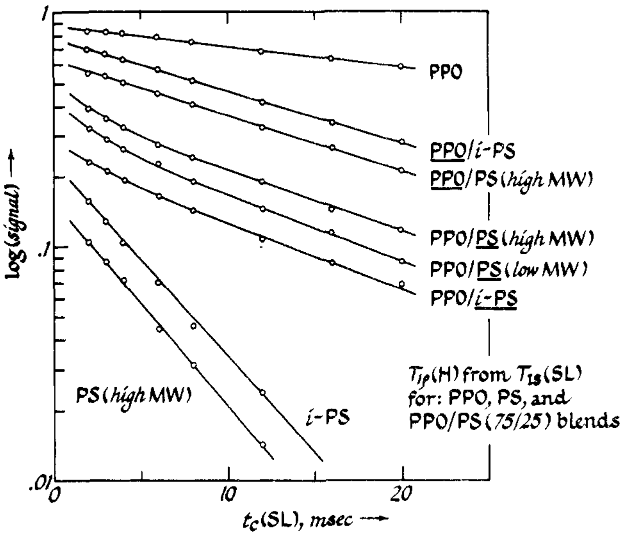

Figure 4. Plots of carbon magnetization generated by long-term matched spin-lock cross-polarization transfers yielding $T_{1\rho}$'s for protons attached to main-chain carbons of PPO, PS, and a variety of 75/25 PPO/PS blends. The pulse sequence of Figure 1 (top) was used.

Table I
Proton $T_{1\rho}$'s of Poly(phenylene oxide)/Polystyrene (75/25) Solid Blends[a,b] (T = 26 °C, H_1 = 37 kHz)

blend	$T_{1\rho}$(H), ms	$\langle T_{1\rho}(\mathrm{H})\rangle$,[c] ms
PPO/*p*-Cl-PS, quenched	48	48
PPO/*p*-Cl-PS, annealed	54	54
PPO/i-PS	20	20
PPO/PS (high MW)	18	22
PPO/PS (low MW)	15	20
PPO/**PS** (high MW)	17	6.8
PPO/**PS** (low MW)	15	6.5
PPO/**i-PS**	15	10
PPO/***p*-Cl-PS**, quenched	9	9.0
PPO/***p*-Cl-PS**, annealed	9	9.0

[a] Boldface identifies the component of the blend whose main-chain proton $T_{1\rho}$ is reported. [b] Estimated accuracy is ±5%. [b] The brackets indicate a nominal initial slope.

Table II
Proton $T_{1\rho}$'s of Some Homopolymers and of Poly(phenylene oxide)/Polystyrene (25/75) Solid Blends[a,b] (T = 26 °C, H_1 = 37 kHz)

system	$T_{1\rho}$(H),[c] ms	$\langle T_{1\rho}(\mathrm{H})\rangle$,[c] ms
PPO	49	49
PPO/PS-d_8	88	88
PPO/PS (high MW)	6.7	6.7
PPO/**PS** (high MW)	6.2	6.2
i-PS	5.3	5.3
PS (high MW)	5.6	5.6
p-Cl-PS	8.0	8.0

[a] Boldface identifies the component of the blend whose main-chain proton $T_{1\rho}$ is reported. [b] Estimated accuracy is ±5%. [c] The brackets indicate a nominal initial slope.

Discussion

Line Shapes. Carbon-13 isotropic chemical shifts arise from relatively short-range effects. The fact that changes in isotropic shifts (or line shapes) of the blends (relative to the component homopolymers) can be observed means that mixing in PPO/PS blends is on an individual chain-for-chain basis. These shifts may be induced either by direct interchain shielding or by indirect conformationally induced effects. In either event, the interacting chains must be nearest neighbors.

Proton–Proton Spin Diffusion in a Two-Component System. The $T_{1\rho}$(H) measurements can tell us something of the homogeneity of intimate PPO/PS blends. However, we must first understand the dynamics of spin diffusion between the PPO and PS protons. We model this relaxation behavior by considering that the protons may be divided into two species, depending on the polymer they are part of (species A for PPO, species B for PS). The equations describing $T_{1\rho}$(H) relaxation in such a system are

$$-\mathrm{d}A/\mathrm{d}t = (K_A + f_Bk_c)A - f_Ak_cB$$

$$-\mathrm{d}B/\mathrm{d}t = (K_B + f_Ak_c)B - f_Bk_cA \qquad (9)$$

where, if n_A and n_B represent the numbers of A and B spins, respectively, $f_A = n_A/(n_A + n_B)$ and $f_B = n_B/(n_A + n_B)$ represent the fractions of A and B spins. The three rate constants K_A (the initial decay rate of PPO protons before cross relaxation makes its influence felt), K_B (the initial decay rate of PS protons), and k_c (the cross-relaxation rate) are defined by

$$K_A = 2n_A\langle W_2\rangle_{AA} + 2n_B\langle W_2\rangle_{AB}$$

$$K_B = 2n_B\langle W_2\rangle_{BB} + 2n_A\langle W_2\rangle_{AB}$$

$$k_c = (n_A + n_B)(\langle W_0\rangle_{AB} - \langle W_2\rangle_{AB}) \qquad (10)$$

In these equations, W_2 represents the probability that a pair of interacting protons will each flip so as to make $\Delta m = \pm 1$ and W_0 represents the probability of a pair of flips resulting in $\Delta m = 0$. The averages are pairwise between spins of the species indicated by the subscripts. There are no terms involving W_1 since $\Delta m = \pm^1/_2$ flips are not important if H_1 is much larger than the local dipolar field.[7] The probabilities $\langle W_0\rangle_{AA}$ and $\langle W_0\rangle_{BB}$ are not small but contribute to neither net relaxation nor cross relaxation and so drop out; they do describe the spin diffusion within species A and B which helps to make it possible to regard each species as homogeneous. These equations are an extension[8] of the treatment of relaxation due to Solomon.[9]

We solve the coupled relaxation equations subject to the initial conditions that $A = A_0$ and $B = B_0$ when $t = 0$. Further we require that $A_0/B_0 = n_A/n_B$. The solution has the form

$$A = a_+e^{r_+t} + a_-e^{r_-t}$$

$$B = b_+e^{r_+t} + b_-e^{r_-t} \qquad (11)$$

where

$$r_\pm = {}^1\!/_2[-(K_A + K_B + k_c) \pm R]$$

$$a_\pm = {}^1\!/_2A_0[1 \pm R^{-1}(K_B + k_c - K_A)]$$

$$b_\pm = {}^1\!/_2B_0[1 \pm R^{-1}(K_A + k_c - K_B)]$$

$$R = +\{[(K_A - K_B) + (f_B - f_A)k_c]^2 + 4f_Af_Bk_c^2\}^{1/2} \qquad (12)$$

As was noted earlier, K_A and K_B represent the initial rates of relaxation. However, as time passes, cross relaxation pulls the relaxation rates together until both A and B relax at the same intermediate rate. Fitting data such as in Figure 4 is simply a matter of determining the initial slopes for each species and then adjusting k_c until the remainder of the decay curves are fitted satisfactorily.

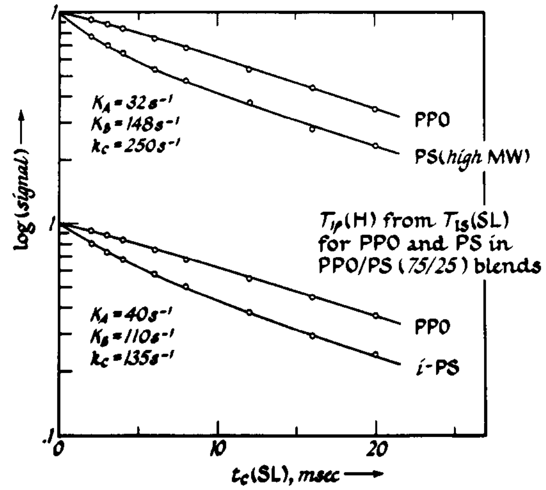

Figure 5. Results of fitting eq 3 to some of the data in Figure 4. The fitting parameters are indicated; the mole fractions used were $f_A = 0.72$ and $f_B = 0.28$. Signal amplitude has been scaled to coincide with the calculated decay curves.

$T_{1\rho}$(H) in the PPO/i-PS Blend. Figure 5 shows the results of fitting the data from two of the blends plotted in Figure 4. Consider first the PPO/i-PS data. The relaxation rate for PPO homopolymer is determined from Figure 4 to be 20 s^{-1}; the rate is 190 s^{-1} for the isotactic PS homopolymer. The values of K_A and K_B required to fit the PPO/i-PS data are clearly intermediate between the homopolymer rates. This suggests that $\langle W_2\rangle_{AB}$ makes a significant contribution to the initial relaxation rates. That is, mixing is intimate enough that PPO relaxation is aided by interaction with nearby, efficiently relaxing PS, and PS relaxation is reduced by its dispersal in PPO.

This explanation is more plausible than one that says that dispersal is not complete but molecular motions are altered by blending. Since $T_{1\rho}$(H) for both PPO and PS is expected to be on the low-temperature side of the $T_{1\rho}$ minimum, an explanation based on changes in motion would require that PS slow down and PPO speed up even though they were not intimately mixed. While, in an intimate mixture, it is possible that some coming together of rates of motion may occur, it is more likely that proton density differences between PPO and PS give rise to the shifts in K_A and K_B on blending. The size of k_c also suggests an intimate mixing of the two species of protons. It is likely that the PS chains are totally separated from one another by PPO.

$T_{1\rho}$(H) in the PPO/PS Blends. When we look at the fit to the PPO/PS (high MW) data in Figure 5 we note something peculiar. Although the fit is as good as to the PPO/i-PS data, the fitting parameters do not seem reasonable when compared to the PPO/i-PS parameters. In PPO/PS (high MW) we have a blend in which K_A and K_B more closely resemble the homopolymer values (as seen in the initial slopes) while k_c indicates greater cross relaxation. The first observation suggests less intimate mixing while the second indicates more intimate mixing.

The increase in k_c cannot be caused by a proton density change since the PPO/i-PS blend is physically the denser of the two. Furthermore, the increase in k_c cannot be attributed to a decrease in $\langle W_2\rangle_{AB}$ as might be suggested by eq 10, since the required large decrease would affect K_A and K_B too much. A decrease in motion could increase

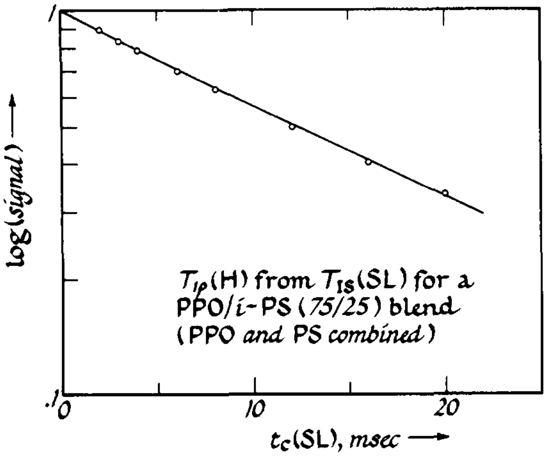

Figure 6. Simulation of a $T_{1\rho}$(H) relaxation decay as would be obtained by direct observation of the composite proton signal. The carbon-derived data (open circles) have been combined with suitable weighting factors. The pair of calculated curves from Figure 5 which fit these data have been combined to yield the (solid) curve shown.

$\langle W_0 \rangle_{AB}$, but then all the $\langle W_2 \rangle$ terms could be expected to decrease for which there is no evidence.

We reconcile this discrepancy by attributing part (perhaps 5–10%) of the initial decay of the PS protons to small regions where the PS is not fully dispersed and hence relaxes more like PS homopolymer. The net result is an effective phase separation and a distribution of PS relaxation rates. This distribution cannot be explained in terms of local statistical fluctuations of homogeneous mixing, since we know[10] that random mixing of PS with proton-deficient perdeuteriopolystyrene results in just a single, average, increased $T_{1\rho}$(H). With an assumption of phase separation for a part of the PPO/PS blend, the relaxation behavior of the remaining part is virtually indistinguishable from that of the PPO/i-PS blend. These regions of poorly dispersed PS need not be more than places where awkwardly kinked atactic PS tends to fold back on itself or where a few independent chains have aggregated. The resulting regions (which may be difficult to detect by neutron scattering[11]) must be in relatively poor contact with nearby PPO chains so that an effective phase separation can occur. The extent of this phase separation could well depend on temperature-dependent subtleties of molding and quenching during processing.[12] We see no evidence for such phase separation in the $T_{1\rho}$(H) results for the 25/75 PPO/PS (high MW) blend (Table II).

Isotactic PS, being more regular than atactic polystyrene, is perhaps less likely to aggregate, or phase separate, on mixing with PPO. Nevertheless, we cannot rule out the possibility that some or all of the curvature in the i-PS relaxation curve is due to such regions. We note, however, that it is *not* necessary to postulate such regions to fit the PPO/i-PS data since the model of cross relaxation we have used fits the shape of the relaxation curves quite well. But, in the event that all of the curvature in the PPO/i-PS relaxation curve is attributable to poorly dispersed i-PS, the behavior of the remaining homogeneous part of the blend does not yield any information about the cross-relaxation process, which actually may be quite fast. The estimated value of k_c of 135 s^{-1} (Figure 5) is therefore a lower limit.

Direct Measurement of $T_{1\rho}$(H). Figure 6 illustrates the point made earlier that the differences we have been discussing would be difficult to discern if the $T_{1\rho}$(H) process were obtained from the total proton signal. While it is true that the quality of proton data in such measurements can be better than our carbon-derived data, the curvature in the combined plot is so slight as to be difficult to characterize. This is because PS in the blend of interest contributes less than a third of the total proton signal.

$T_{1\rho}$(H) in Immiscible Blends. We have emphasized in this Discussion the characterization of small regions of heterogeneities in what is primarily a homogeneous solid blend. Our NMR technique, however, is equally well suited to the detection of small regions of apparently intimate mixing in what is primarily an inhomogeneous blend of immiscible components. Thus, the similarity of $T_{1\rho}$(H)'s for PPO in the homopolymer and in the 75/25 blend with poly(*p*-chlorostyrene) (Tables I and II) is strong evidence for the absence of any significant interchain mixing, even in the quenched material. Since prolonged annealing of the blend tends to increase only the PPO $T_{1\rho}$(H), we suspect that this modest increase is due to changes in low-frequency molecular motions within the PPO domains and to possible changes in interfacial contact.

References and Notes

(1) Schaefer, J.; Stejskal, E. O.; Buchdahl, R. *Macromolecules* **1977**, *10*, 384.
(2) For example: MacKnight, W. J.; Karasz, F. E.; Fried, J. R. In "Polymer Blends"; Paul, D. R., Newman, S., Eds.; Academic Press: New York, 1977.
(3) Schaefer, J.; Sefcik, M. D.; Stejskal, E. O.; McKay, R. A. *Polym. Prepr., Am. Chem. Soc., Div. Polym. Chem.* **1979**, *20*, 247.
(4) Stejskal, E. O.; Schaefer, J. *J. Magn. Reson.* **1975**, *18*, 560.
(5) Stejskal, E. O.; Schaefer, J.; Steger, T. R. *Symp. Faraday Soc.* **1979**, *13*, 56.
(6) McCall, D. W. *Acc. Chem. Res.* **1971**, *4*, 223.
(7) Jones, G. P. *Phys. Rev.* **1966**, *148*, 332.
(8) Brooks, A. A.; Cutnell, J. D.; Stejskal, E. O.; Weiss, V. W. *J. Chem. Phys.* **1968**, *49*, 1571.
(9) Solomon, I. *Phys. Rev.* **1955**, *99*, 559.
(10) Schaefer, J.; Sefcik, M. D.; Stejskal, E. O.; McKay, R. A. *Macromolecules* **1981**, *14*, 188.
(11) Wignall, G. D.; Child, H. R.; Li-Aravena, F. *Polymer* **1980**, *21*, 131.
(12) Comment by Professor F. E. Karasz (University of Massachusetts) in the discussion of this paper following presentation at the symposium "Multi-Component Polymer Systems", University of Cincinnati, Dec 10, 1979.